two ions. The DFS-encoded state can store a qubit at least 10 times as long under applied noise as a single ion can, and appears immune to collective dephasing. Under typical ambient conditions, the DFS encoding also improves storage time considerably, showing that collective dephasing is indeed the limit to quantum memory using our physical qubits. Even without normalizing for the overhead incurred in encoding and decoding, the encoded state retains more coherence than the test state for long storage times in ambient conditions. The DFS encoding therefore currently provides an improved single-qubit quantum memory for ion-trap quantum computing applications. The loss of coherence incurred in encoding and decoding is a drawback to our scheme, but in the future, practical quantum computing will in any case require logic gates of a much higher fidelity than those used in this work. We therefore expect that, once the technical problems of ion heating and laser fluctuations are solved, the scheme presented here should be a practical method for long-term storage of qubits with near-perfect fidelity.

Our results suggest applications in quantum communication and large-scale quantum computing. Single photons have already been shown to transmit quantum information over long distances with high fidelity (*8, 9*), and the information in a single photon can be mapped onto a single atom (*28, 29*). With our encoding technique, the quantum information received by a single ion can be mapped into a DFS for robust storage. Our encoding technique will also be essential in scaling up ion-trap quantum computers. In one model of large-scale ion-trap quantum computing (*19*), qubits reside in a large array of interconnected ion traps. To perform one- or two-qubit logic gates, the relevant ions are moved into "accumulator" regions where they interact with lasers that drive the gates. One obstacle to this quantum computing architecture is that the magnetic field strength must be well-characterized across the entire device. Otherwise, the ions will constantly accumulate unknown relative phase during transport, leading to decoherence. Encoding into the DFS solves this problem, because the phase of a logical qubit in the DFS does not depend on the local magnetic field strength as long as the field strength is the same at each physical qubit. Thus, we can entangle two logical qubits, move them far apart, and perform operations on them in separate accumulators without losing phase information.

References and Notes

1. P. W. Shor, in *Proceedings of the 35th Annual Symposium on Foundations of Computer Science*, S. Goldwasser, Ed. (IEEE Computer Society, Los Alamitos, CA, 1994), p. 116.
2. L. K. Grover, *Phys. Rev. Lett.* **79**, 325 (1997).
3. A. Steane, paper presented at the Fifth International Conference on Quantum Communication, Measurement, and Computing, Capri, Italy, 3 to 8 July 2000.
4. W. H. Zurek, *Phys. Today* **44** (no. 10), 36 (1991).
5. D. Giulini *et al.*, *Decoherence and the Appearance of a Classical World in Quantum Theory* (Springer, Berlin, 1996).
6. G. M. Palma, K.-A. Suominen, A. K. Ekert, *Proc. R. Soc. London Ser. A* **452**, 567 (1996).
7. P. Zanardi, F. Rossi, *Phys. Rev. Lett.* **81**, 4752 (1998).
8. *Fortschr. Phys.* **46** (no. 4-8) (1998).
9. *Fortschr. Phys.* **48** (no. 9-11) (2000).
10. D. A. Lidar, I. L. Chuang, K. B. Whaley, *Phys. Rev. Lett.* **81**, 2594 (1998).
11. P. Zanardi, M. Rasetti, *Phys. Rev. Lett.* **79**, 3306 (1997).
12. L. M. Duan, G. C. Guo, *Phys. Rev. A* **57**, 737 (1998).
13. D. A. Lidar, D. Bacon, K. B. Whaley, *Phys. Rev. Lett.* **82**, 4556 (1999).
14. D. Bacon, J. Kempe, D. A. Lidar, K. B. Whaley, *Phys. Rev. Lett.* **85**, 1758 (2000).
15. A. Beige, D. Braun, B. Tregenna, P. L. Knight, *Phys. Rev. Lett.* **85**, 1762 (2000).
16. P. G. Kwiat, A. J. Berglund, J. B. Altepeter, A. G. White, *Science* **290**, 498 (2000).
17. Q. A. Turchette *et al.*, *Phys. Rev. A* **61**, 063418 (2000) (available at http://publish.aps.org/abstract/PRA/v61/e063418).
18. The hyperfine states corresponding to $|\downarrow\rangle$ and $|\uparrow\rangle$ are the $|F = 2, m_F = -2\rangle$ and $|F = 1, m_F = -1\rangle$ sublevels of the ground $^2S_{1/2}$ state, respectively. The cycling transition is excited by left circularly polarized light and connects $|\downarrow\rangle$ to the $|F = 3, m_F = -3\rangle$ sublevel of the excited $^2P_{3/2}$ state.
19. D. J. Wineland *et al.*, *J. Res. NIST* **103**, 259 (1998).
20. For two ions, we effect common-mode changes of ϕ_1 and ϕ_2 by changing the phase of the RF synthesizer that controls the difference frequency $\omega_{BR} - \omega_{RR}$. By changing the oscillation frequency of the trap, we can control the ion spacing precisely, allowing us to make differential changes to ϕ_1 and ϕ_2. These two techniques combined allow us to control ϕ_1 and ϕ_2 independently for two ions.
21. C. A. Sackett *et al.*, *Nature* **404**, 256 (2000).
22. A. Sørensen, K. Mølmer, *Phys. Rev. A* **62**, 022311 (2000) (available at http://publish.aps.org/abstract/PRA/v62/e022311).
23. _____, *Phys. Rev. Lett.* **82**, 1971 (1999).
24. Individual optical addressing of the ions can prepare the desired state with only one carrier pulse [H. C. Nägerl *et al.*, *Phys. Rev. A* **60**, 145 (1998)], but it is technically more challenging in our experiment because our ions are separated by only ~2.5 μm.
25. The decoding and final rotation can give rise to coherence in ion 2 even if the state before decoding is completely incoherent. We avoid this eventuality by detuning the RF synthesizer used for the initial and final rotations of ion 2 from the synthesizers used for encoding and decoding. The phases α and α' then change from shot to shot of the experiment, and the spurious coherences average out over many shots. No trace of this effect then remains in the data.
26. We can also reduce the dephasing from this mechanism by using the $^2S_{1/2}$ hyperfine sublevels $|F = 1, m_F = 0\rangle$ and $|F = 2, m_F = 0\rangle$ to represent the two levels of a qubit. In a separate experiment, we measured the coherence time of superpositions of these two states at a static magnetic field of $\sim 1.6 \times 10^{-3}$ T to be an order of magnitude longer than the coherence time between the qubit basis states used here. Magnetic field dephasing still limits the coherence time between the $m_F = 0$ states through the quadratic Zeeman shift. We expect the DFS encoding to improve coherence time in this case as well, because the encoding protects against purely collective dephasing to all orders. A practical ion-trap quantum computer will probably use the $m_F = 0$ states as qubit basis states but will also encode qubits into the DFS.
27. B. E. King *et al.*, *Phys. Rev. Lett.* **81**, 1525 (1998).
28. X. Maitre *et al.*, *Phys. Rev. Lett.* **79**, 769 (1997).
29. J. I. Cirac, P. Zoller, H. J. Kimble, H. Mabuchi, *Phys. Rev. Lett.* **78**, 3221 (1997).

30. This work was supported by the U.S. National Security Agency and the Advanced Research and Development Activity under contract MOD-7171.00 and by the U.S. Office of Naval Research. We thank J. Bergquist and A. Ben-Kish for comments on the manuscript. This paper is a contribution of the National Institute of Standards and Technology and is not subject to U.S. copyright.

10 November 2000; accepted 22 December 2000
Published online 5 January 2001;
10.1126/science.1057357
Include this information when citing this paper.

Magnetization Precession by Hot Spin Injection

W. Weber,[1]* S. Riesen,[1] H. C. Siegmann[2]

As electrons are injected at various energies into ferromagnetic material with their spin polarization vector perpendicular to the axis of the magnetization, we observe precessional motion of the spin polarization on the femtosecond time scale. Because of angular momentum conservation, the magnetization vector must precess as well. We show that spin injection will generate the precessional magnetization reversal in nanosized ferromagnetic bits. At reasonable injected current densities this occurs on the picosecond time scale.

Electrons injected into ferromagnetic material experience exchange coupling to the magnetization and spin-dependent scattering, leading to excitations of the magnetization (*1–4*). By injecting currents of high density, these excitations have been observed through the occurrence of spin waves (*5–7*), permanent changes of the micromagnetic structure (*8*, *9*), or even a reversal of the magnetization (*10–12*). However, to date, the injection of electrons from a ferromagnetic emitter through nanocontacts occurs continously or in pulses that are long compared with the relaxation

[1]Laboratorium für Festkörperphysik, ETH Zürich, CH-8093 Zürich, Switzerland. [2]Stanford Linear Accelerator Center, Stanford University, Stanford, CA 94309, USA.

*To whom correspondence should be addressed. E-mail: weber@solid.phys.ethz.ch

of the magnetization vector **M** into the direction of the effective field, meaning that precession and relaxation of **M** are intertwined. Furthermore, the spin polarization **P** of the injected electrons is not known. This arises because **P** is modified and may even change sign in the process of extracting the electrons from the ferromagnet (*13–15*). All this comes together to make it impossible to uniquely interpret the existing experiments in terms of specific elementary processes.

We present an experiment in which these disadvantages are avoided and in which the precession of the magnetization by hot spin injection can be measured. We also provide comprehensive results for the elemental ferromagnets Fe, Co, and Ni. It turns out that high precession frequencies equivalent to the application of a magnetic field of ~1 T may be generated at reasonable injected current densities in Fe, Co, and Ni, suggesting that the spin-injection technique may be suitable to technically relevant materials for precessional magnetization reversal. The precession mode of reversal is an attractive concept for advancing the speed of magnetic data recording into the picosecond time scale (*16*). The current-induced switching as practised at present and as discussed in (*1*) is different in that it uses both precession and relaxation of the magnetization, yet it has a fundamental time barrier of about 1 ns imposed by the spin-lattice relaxation below which it cannot be effectuated. Precessional reversal, on the other hand, has no such time barrier, as explained in more detail in (*16*) and below.

The principle of the present experiment is that an ensemble of spin-polarized electrons is introduced into the ferromagnet. The spin polarization vector $\mathbf{P}_0$ of the ensemble at the time $t = 0$ encloses an angle $\vartheta = \pi/2$ with the magnetization **M**. After the electrons have spent a time t on the order of a few femtoseconds within the ferromagnet, **P** is measured again. One finds that **P** has precessed about an axis parallel to **M** by an angle ϵ, and that **P** has rotated into **M**, reducing the angle ϑ. The precession angle $\epsilon = \Delta E \cdot t/\hbar$ is due to the exchange splitting ΔE of the electron states in the ferromagnet, whereas the rotation into **M** is caused by the spin-dependent scattering of the electrons (*17*, *18*). The finding that ϑ is always reduced means that the minority spins are scattered more strongly compared with the majority spins (*19*). Note that we define the direction of **M** by the direction of the majority spins in the ferromagnet.

Once an electron has crossed the surface barrier potential and is inside the ferromagnet, we have a closed system with no external forces. Hence, the total angular momentum **L**, consisting of the angular momentum of the magnetization $\mathbf{L}_M$ and the one of the injected spins $\mathbf{L}_e$, is conserved. It follows that the total torque $\boldsymbol{T} = d\boldsymbol{L}/dt = 0$. The observed precession of **P** means that **M** produces a torque $\mathbf{T}_e$ on the injected electrons. Hence, these electrons must also produce in turn a torque $\mathbf{T}_M$ on **M** with $\boldsymbol{T} = \boldsymbol{T}_e + \boldsymbol{T}_M = 0$. Therefore, by measuring the torque $\mathbf{T}_e$, we have also measured $\mathbf{T}_M$. Finally, from $\mathbf{T}_M$, one obtains the precession frequency ω_M of the magnetization. This precession is generated by the nonequilibrium exchange interaction of the injected spins (*20*) and is the essential ingredient in the reversal mode discussed here as previously shown (*21*).

The rotation of **P** into **M** produces no torque; however, it leads to an increase of the magnitude of the angular momentum of the injected electrons parallel to **M**. Hence, $|\boldsymbol{M}|$ must decrease correspondingly to conserve **L**. This occurs by scattering of electrons into the holes of the *d* shell, producing localized excitations that later may decay into spin waves. These types of excitations occur also when initially unpolarized electrons or electrons with $\mathbf{P}_0$ antiparallel to **M** are introduced into the ferromagnet. On the other hand, precession always requires a component of the injected spin polarization perpendicular to **M**.

In practice, the experiment is done by letting a spin-polarized, low-energy electron beam produced in a GaAs photocathode pass through a ferromagnetic film of thickness d on the order of a few nanometers. The femto- and subfemtosecond time scale is accessible because the electrons typically require fractions of a femtosecond to traverse 1 nm. The polarization is measured on those electrons that have traversed the ferromagnetic film without losing energy (the energy resolution of the retarding field analyzer is 0.5 eV full width at half maximum). Of course, the ferromagnetic film is too thin to stand alone; rather, it has to be supported by a polycrystalline gold foil of about 20-nm thickness and furthermore capped for chemical protection by yet another gold film of 2-nm thickness. The most difficult task is to avoid pinholes in the trilayer structure. Even the tiniest pinhole will increase the transmitted current, thereby reducing or even swamping the observations of the transmitted spin polarization. One of the essential advantages of the present experiment compared with all-solid-state structures is that the trilayer can be checked independently for pinholes by increasing the electron energy to around 30 eV. Owing to onset of the scattering with the 5*d* electrons in Au, the transmitted current must vanish at these energies in the absence of pinholes. The fabrication of the trilayers Au/ferromagnet/Au is described elsewhere (*17*, *22*).

The dependence of the precession angle ϵ on the film thickness d for Fe, Co, and Ni is shown in Fig. 1 and is valid for elastic electrons at 7 eV above the Fermi energy E_F. The data point at $d = 0$ was taken with the Au substrate alone, showing that **P** does not precess in Au as expected. A linear fit describes the observations in all three ferromagnets, indicating that the precession is a bulk property of the ferromagnets. The slope is the specific precession angle $\tilde{\epsilon} = 33°/\text{nm}$, 19°/nm, and 7°/nm for Fe, Co, and Ni, respectively. However, the linear fits intercept the abscissa at finite thicknesses $d_0 > 0$, an indication that the two interfaces of the ferromagnet with Au of joint thickness d_0 do not contribute to the precession. Reasons for this include both the absence or weakening of the magnetization by interdiffusion and the nonuniformity of the ferromagnetic-film thickness (*23*). We do not discuss the reasons for the occurrence of d_0 in more depth because we are focusing here on bulk effects of the ferromagnet as extracted with the specific precession angle $\tilde{\epsilon}$.

If v is the group velocity of the electrons in the ferromagnet, the precession frequency of the electrons is $\omega_e = \tilde{\epsilon}\, v$. With the

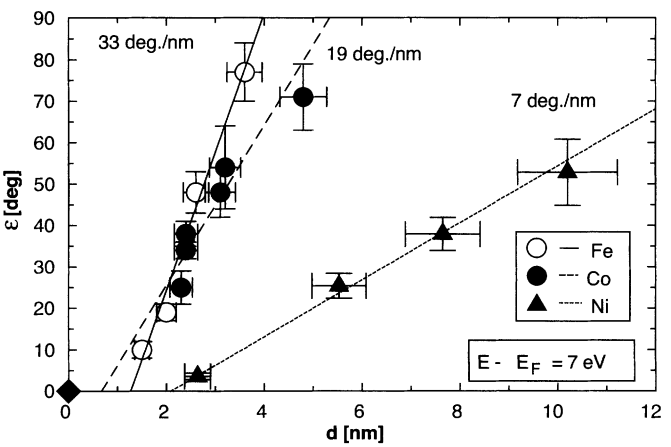

Fig. 1. The spin precession angle ϵ as a function of the ferromagnetic-film thickness for Fe, Co, and Ni, measured with elastic electrons of energy $(E - E_F) = 7$ eV. The point at zero thickness was measured with a pure Au film 20-nm thick. The straight lines through the data points represent linear fits.

current density $j = n_e ev$ of the injected electrons, where n_e is the electron density and e the elementary charge, the torque (per unit volume) acting on the injected spins is $T_e = \omega_e L_e \sin\vartheta = P_0 n_e \omega_e (\hbar/2) \sin\vartheta = (\hbar/2e) P_0 j \tilde{\epsilon} \sin\vartheta$. On the other hand, the torque (per unit volume) acting on the magnetization is $T_M = \omega_M L_M \sin\vartheta$. With $T_M = T_e$, the precession frequency of **M** is then obtained from

$$\omega_M = P_0 j \tilde{\epsilon} / e n_M n_B \quad (1)$$

where n_B is the number of Bohr magnetons per atom and n_M is the density of the atoms in the ferromagnet. For simplicity, we have neglected the orbital contribution to the magnetization by setting the angular momentum (per unit volume) $L_M = n_B n_M \hbar/2$. Assuming $j = 10^{13}$ A/m^2, as reported for nanocontacts (*9*, *12*), Eq. 1 yields $\omega_M = 1.94 \times 10^{11}$, 1.35×10^{11}, and 1.4×10^{11} s^{-1} for Fe, Co, and Ni with the respective specific precession angles $\tilde{\epsilon}$ from Fig. 1 and assuming $P_0 = 1$. These precession frequencies are obtained exclusively from experimental data. They correspond to the application of a magnetic field of 1.1, 0.76, and 0.79 T. Considering the large differences between Co and Ni in $\tilde{\epsilon}$, it is perhaps surprising that ω_M is nevertheless the same. This arises because the exchange field produced by one Bohr magneton is similar in the different ferromagnets, which is then reflected in the finding that $\tilde{\epsilon}/n_B$ does not vary by much.

The spin polarization vector **P** relaxes into the direction of **M**. The experiments show that this relaxation takes a few femtoseconds only. The data for the angle ϑ enclosed by **P** and **M** (Fig. 2) are given as a function of the thickness d of the Fe, Co, and Ni films. The decrease of ϑ with increasing d is due to the well-known spin-selective inelastic scattering, i.e., the preferential absorption of minority spins in the ferromagnet. It is evident that spin-selective inelastic scattering is similar in Fe and Co but less effective in Ni. The curves through the data points represent fits based on the results from physically very different experiments (*19*). In these experiments, one measures the attenuation of a spin-polarized electron beam with intensities $I^+ = I_0 \exp(-\sigma^+ d)$ at $\mathbf{P}_0$ parallel to **M** and with $I^- = I_0 \exp(-\sigma^- d)$ at $\mathbf{P}_0$ antiparallel to **M**. The spin asymmetry of electron absorption is $A = (I^+ - I^-)/P_0(I^+ + I^-) = \{\exp[(\sigma^- - \sigma^+)d] - 1\}/P_0\{\exp[(\sigma^- - \sigma^+)d] + 1\}$, where σ^+ and σ^- are the absorption coefficients of majority and minority spins, respectively. Elementary theory shows that $\vartheta = \arctan(P_0 \sqrt{1 - A^2}/A)$. We see that the present data agree well with previous experiments obtained by measuring A. Again, ϑ reaches its initial value of 90° at finite film thicknesses. These d_0 values up to which no rotation of **P** occurs are similar to those for the absence of precession, indicating that their occurrence is due to the reduction or absence of magnetization at the two interfaces. The important observation is that the precession of **P** about **M** or vice versa of **M** about **P** on a cone with large opening angle ϑ will only occur over a short distance of a few nm from the point of injection of the spin-polarized electrons.

M relaxes also into **P**, but this relaxation is much slower. The relaxation time of **M** into the direction of a field is obtained from experiments determining the damping parameter in the Landau-Lifshitz-Gilbert equation (*16*), or from the width of the ferromagnetic resonance, or directly by time-resolved images of the magnetization precession (*24*). The relaxation time of **M** into the direction of an applied field turns out to be 0.1 to 1 ns. In thin films, it is mainly due to the excitation of spin waves. This explains why the relaxation of **M** is so much slower than the relaxation of **P** into **M**, which is caused by electron scattering.

Furthermore, the axis of precession of **M** changes direction in space as the injected electrons travel through the ferromagnet. This arises because the torque $\boldsymbol{T}_e = -\boldsymbol{T}_M$ is always perpendicular to **P** and **M**. Hence, while **P** precesses about an axis parallel to **M**, **M** in turn must precess about an axis parallel to **P**, which precesses itself at the frequency ω_e. To obtain a nonvanishing precession component of **M** along a direction fixed in the lattice of the ferromagnet, the ferromagnetic-film thickness must be small relative to the path length on which **P** precesses itself by 2π. This is yet another, although less critical, reason why the sample thickness is important for the observation of magnetization reversal by spin injection.

The dependence of the precession angle ϵ on electron energy may be determined in the present experiment as well (Fig. 3). In the case of Co and Ni, the variation of ϵ in the energy range of 5 to 12 eV above E_F is weak; ϵ decreases somewhat, in agreement with $\epsilon = \Delta E \cdot t/\hbar$, because the time t spent by the electrons within the ferromagnet decreases with $1/\sqrt{E}$). Thus, the exchange energy ΔE in the polycrystalline samples is

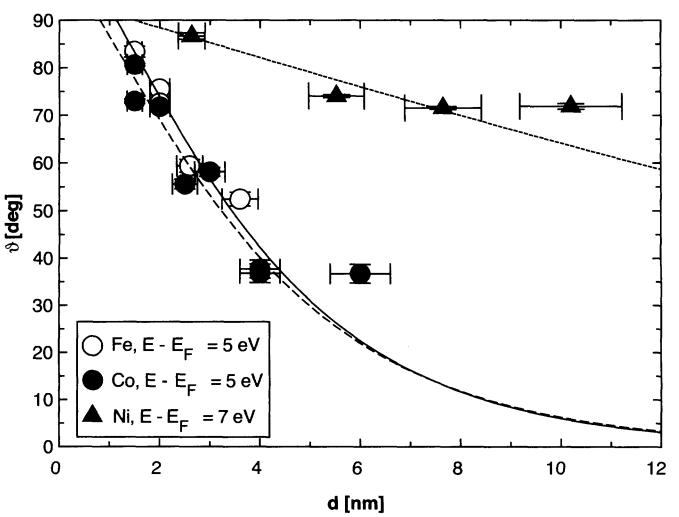

Fig. 2. The angle ϑ enclosed by **P** and **M** as a function of the ferromagnetic-film thickness for Fe, Co, and Ni, measured with elastic electrons of energy $(E - E_F) = 5$ and 7 eV. The values of the angle ϑ are normalized to $P_0 = 1$ (pure spin state). The curves through the data points represent fits that are based on results obtained in a number of different experiments (*19*) (Fe: continuous line, Co: dashed line, Ni: dotted line).

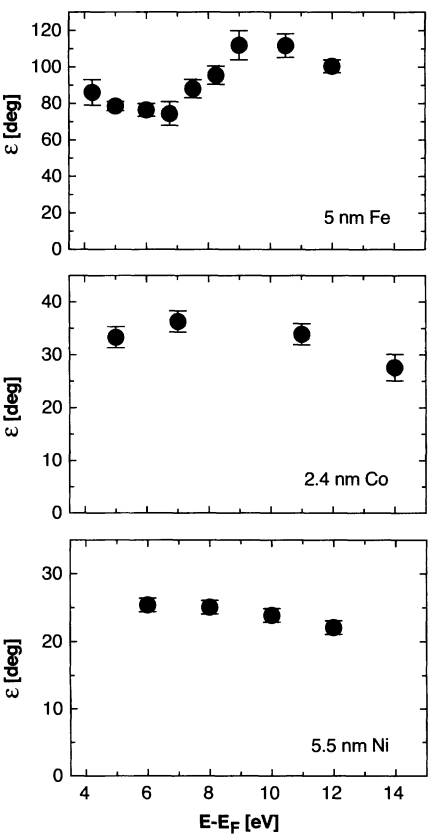

Fig. 3. The spin precession angle ϵ at constant film thickness as a function of the electron energy for Fe (top), Co (middle), and Ni (bottom).

quite constant, extending to surprisingly high electron energies. This finding agrees with predictions from band structure calculations. In the case of Fe, ϵ exhibits a much stronger dependence on electron energy, with a maximum at 9 eV above E_F (*25*). This agrees well with the band structure showing flattening of the bands at this energy and thus a decrease of the group velocity of the electrons (*26*). The time spent by the electrons within the ferromagnet is thus not simply proportional to the thickness d of the ferromagnet, as in the free-electron model used so far, but rather depends on the group velocity. One expects further corrections at energies where the electrons can form quantum-well states in the ferromagnetic film. However, this requires single-crystalline samples of uniform thickness that could not be observed with the present polycrystalline films.

The most appropriate electron energies are at around 1 eV above E_F for the application of spin injection in devices based on the combination of ferromagnetic metals and semiconductor materials. However, so far the precession angle ϵ has not been measured at energies below the vacuum energy. There is no principal obstacle against using an all-solid-state device with two ferromagnetic films before and after the sample under investigation, one film acting as a source and the other as a detector of the spin polarization (*27*). On the basis of the well-established spin-polarized band structure of the ferromagnetic metals, it is likely that ϵ will increase on approaching E_F. Indeed, it has been reported (*11*) that an effective field equivalent to 100 to 200 Oe is generated in Ni wires by drawing a spin-polarized current of 10^{11} A/m^2. This effective field is about twice the one calculated from Eq. 1 when the specific precession angle observed at electron energies of 7 eV above E_F is used. However, this experiment (*11*) cannot rigorously be compared to the present experiment because the injected current lasted 200 ns, which is much longer than the relaxation time of **M** into the direction of the effective field produced by the injected electrons. Another major point is the very fast relaxation of **P** into **M** (Fig. 2). In this instance, experimental results are available at the lower electron energies (*28*, *29*) showing that the inelastic lifetimes of the electrons increase on approaching E_F. Hence, spin relaxation is expected to slow on lowering the electron energy. Using low-energy electrons in solids will generally make it easier to induce precession of **M**. An accurate quantitative description of a solid-state device needs the consideration of spin-dependent interface scattering (*1*), multiple reflections, and interference of electron waves from the various interfaces within the device (*30*). We have only considered the phenomena induced by the electrons once they are inside the ferromagnet. The data in Figs. 1 and 2 justify the assumption of the relative weakness of interface scattering effects in the present setup. Furthermore, the electrons in a solid-state device will not be collimated as in our scattering experiment, but will impinge on the ferromagnetic film from a wider distribution of angles.

Precessional magnetization reversal is much simpler to achieve than the thermally assisted magnetization reversal, in which the external field is applied antiparallel to **M** and in which curling or buckling modes as well as domain-wall motion and pinning of **M** by defects may occur. Precessional reversal is accurately described by the Landau-Lifshitz-Gilbert equation involving only two material parameters, the anisotropy and the damping of the precession of **M**. Two conditions are essential to achieve precessional reversal: first, the external magnetic field $\mathbf{B}_{ext}$ must come in a pulse shorter than the relaxation time of **M** into $\mathbf{B}_{ext}$, which is on the order of 0.1 to 1 ns; and second, $\mathbf{B}_{ext}$ must be perpendicular to **M**. In this way, **M** experiences maximum torque and precesses around $\mathbf{B}_{ext}$. The magnetic field pulses of the Oerstedt type produced in the laboratory frame by the highly relativistic electron bunches delivered from an accelerator are ideal to fulfill these conditions (*31*). The most favorable materials are in-plane magnetized uniaxial thin films (*16*), in which $\mathbf{B}_{ext}$ is applied in the plane of the film. **M** then precesses out of the plane of the film, thereby producing a demagnetizing field; the precession of **M** around this field completes the reversal after $\mathbf{B}_{ext}$ has ceased to exist. Generally, the angle ϵ_M by which **M** must precess out of the film plane before $\mathbf{B}_{ext}$ can be switched off depends on the properties of the material; $\epsilon_M = 20°$ is sufficient to trigger the reversal in a Co film.

The question then is whether a spin-polarized current can produce such precession angles ϵ_M. From Eq. 1, one finds that with $P_0 = 1$ and $j = 10^{13}$ A/m^2, a duration of the injected pulse of $\tau_{pulse} = \epsilon_M/\omega_M = 2$ ps is sufficient. With the more realistic $P_0 = 0.3$ for ferromagnetic emitters, $\tau_{pulse} = 6$ ps. Smaller injected current densities may be compensated for by increasing τ_{pulse}; however, the pulse length must remain below the relaxation time of **M**. Hence, the essential conditions for inducing precessional reversal are very thin ferromagnetic samples of a few nanometers thickness, the injection of an electron current with a component of spin polarization perpendicular to **M**, and a duration of the injection below 0.1 ns. This shows that hot spin injection can readily induce precessional magnetization reversal (*32*).

References and Notes

1. J. C. Slonczewski, *J. Magn. Magn. Mater.* **159**, L1 (1996).
2. L. Berger, *Phys. Rev. B* **54**, 9353 (1996).
3. Y. B. Bazaliy, B. A. Jones, S.-C. Zhang, *Phys. Rev. B* **57**, R3213 (1998).
4. J. Z. Sun, *Phys. Rev. B* **62**, 570 (2000).
5. M. Tsoi *et al.*, *Phys. Rev. Lett.* **80**, 4281 (1998).
6. S. M. Rezende, F. M. de Aguiar, M. A. Lucena, A. Azevedo, *Phys. Rev. Lett.* **84**, 4212 (2000).
7. M. Tsoi *et al.*, *Nature* **406**, 46 (2000).
8. E. B. Myers, D. C. Ralph, J. A. Katine, R. N. Louie, R. A. Buhrman, *Science* **285**, 867 (1999).
9. N. Garcia, H. Rohrer, I. G. Saveliev, Y.-W. Zhao, *Phys. Rev. Lett.* **85**, 3053 (2000).
10. J. Z. Sun, *J. Magn. Magn. Mater.* **202**, 157 (1999).
11. J.-E. Wegrowe, D. Kelly, Y. Jaccard, Ph. Guittienne, J.-Ph. Ansermet, *Europhys. Lett.* **45**, 626 (1999).
12. J. A. Katine, F. J. Albert, R. A. Buhrmann, E. B. Myers, D. C. Ralph, *Phys. Rev. Lett.* **84**, 3149 (2000).
13. M. Sharma, S. X. Wang, J. H. Nickel, *Phys. Rev. Lett.* **82**, 616 (1999).
14. J. M. De Teresa *et al.*, *Science* **286**, 507 (1999).
15. J. S. Moodera, J. Nowack, L. R. Kinder, P. M. Tedrow, *Phys. Rev. Lett.* **83**, 3029 (1999).
16. C. H. Back *et al.*, *Science* **285**, 864 (1999).
17. D. Oberli, R. Burgermeister, S. Riesen, W. Weber, H. C. Siegmann, *Phys. Rev. Lett.* **81**, 4228 (1998).
18. W. Weber, D. Oberli, S. Riesen, H. C. Siegmann, *N. J. Phys.* **1**, 9.1 (1999).
19. H. C. Siegmann, in *Selected Topics on Electron Physics*, M. Campbell, H. Kleinpoppen, Eds. (Plenum, New York, 1996), pp. 221–231.
20. C. Heide, R. J. Elliott, *Europhys. Lett.* **50**, 271 (2000).
21. C. Heide, P. E. Zilberman, R. J. Elliott, *arXiv cond–mat*, 0005064 (2000); available at http://arXiv.org/abs/cond-mat/0005064.
22. S. Riesen, thesis, ETH Zürich (2001).
23. We note that a nonuniformity of the ferromagnetic-film thickness only influences the d_0 values, whereas the specific precession angles $\tilde{\epsilon}$ are not affected. We find a thickness variation with a root-mean-square value of about 0.5 nm for all three ferromagnets.
24. Y. Acremann *et al.*, *Science* **290**, 492 (2000).
25. The data points for Fe in the energy range around $(E - E_F) = 7$ eV cannot be compared with the ones of Fig. 1. This arises because the Au/5 nm Fe/Au trilayer was subject to excessive sputtering, leading to a reduction of the magnetization. This was necessary to enable measurements of the spin polarization up to electron energies of 12 eV above E_F.
26. E. Colavita *et al.*, *Phys. Rev. B* **25**, 2490 (1982).
27. L. Berger, *IEEE Transact. Magn.* **31**, 3871 (1995).
28. M. Aeschlimann *et al.*, *Phys. Rev. Lett.* **79**, 5158 (1997).
29. W. H. Pippard, R. A. Buhrman, *Phys. Rev. Lett.* **84**, 971 (2000).
30. X. Waintal, E. B. Myers, P. W. Brouwer, D. C. Ralph, *Phys. Rev. B* **62**, 12317 (2000).
31. H. C. Siegmann *et al.*, *J. Magn. Magn. Mater.* **151**, L8 (1995).
32. The maximum of the Oerstedt type of field produced by injecting the current density j is $H_{max} = D \cdot j/4$, where D is the diameter of the nanocontact. The precession frequency of **M** produced by this field is always small compared with ω_M in Eq. 1 for nanocontacts with $D \leq 100$ nm.

33. We gratefully acknowledge financial support by the Swiss National Science Foundation.

14 November 2000; accepted 10 January 2001